Advancing surgical cutting guide flexibility: A hybrid physical and Augmented Reality solution for cranio-maxillofacial surgery

Journal of Cranio-Maxillo-Facial Surgery 54 (2026) 104480

Contents lists available at ScienceDirect

Journal of Cranio-Maxillo-Facial Surgery

journal homepage: www.jcmfs.com

Advancing surgical cutting guide flexibility: A hybrid physical and Augmented Reality solution for cranio-maxillofacial surgery

Federico Salerno *, Luca Ulrich, Giorgia Marullo, Sandro Moos, Enrico Vezzetti

Department of Production and Management Engineering, Politecnico di Torino, Corso Duca degli Abruzzi, 24, Turin, 10129, Italy

ARTICLE INFO

Keywords:
Adjustable surgical guide
Augmented Reality
Hololens 2
Pose estimation
Cranio-maxillofacial surgery
Hybrid surgical guide

ABSTRACT

Cutting guides are widely used in cranio-maxillofacial surgery by providing mechanical references for precise bone resections and reducing intraoperative variability. Nevertheless, their rigid and patient-specific design requires dedicated CAD modeling and fabrication, making them time-consuming to produce and difficult to adapt when anatomical conditions or bone surfaces change. This work presents a hybrid surgical cutting guide that combines a physically adjustable device with Augmented Reality (AR) feedback to support intraoperative alignment in maxillofacial osteotomies. The concept merges the tactile reliability of conventional guides with the adaptability of digital visualization, enabling surgeons to fine-tune the cutting plane directly through AR tracking. Registration was performed using cephalometric landmarks and an inside-out tracking approach with HoloLens 2, allowing precise superimposition of virtual cutting planes onto 3D-printed mandibular models. The system was evaluated by both expert and novice operators under three feedback conditions: no AR, holographic overlay, and real-time distance guidance. Results showed that AR feedback was associated with improved positional accuracy, with mean linear deviations of 1.27 ± 0.71 mm and angular errors of $4.46 \pm 3.27°$. Operator experience influenced overall performance, yet enhanced feedback compensated part of this variability. Combining physical and digital guidance can yield more adaptable, precise, and reusable osteotomy tools, paving the way for flexible surgical assistance in clinical settings.

1. Introduction

Osteotomies are fundamental procedures in cranio-maxillofacial surgery, enabling precise bone cutting to correct structural abnormalities, restore function, and manage traumatic or pathological conditions when conservative treatments are insufficient (Pavlíková et al., 2011; Tache and Mommaerts, 2020; Salerno et al., 2023). They are routinely applied in orthognathic surgery, trauma reconstruction, and oncological resections, where accuracy is critical to achieving both functional and aesthetic outcomes (Chang et al., 2003; Ohba et al., 2017; Weiss II et al., 2021). Given the complex anatomy of the craniofacial region, the success of these procedures strongly depends on careful preoperative planning and accurate intraoperative execution (Westermark et al., 2005; Xue et al., 2018).

Traditionally, osteotomies have been performed using a free-hand approach based on the surgeon's experience and anatomical knowledge (Sunil et al., 2006). While this technique offers flexibility and a straightforward workflow, it is inherently dependent on manual skill and lacks objective intraoperative feedback, which may lead to variability and reduced reproducibility, particularly in complex cases (Kommers et al., 2014; Bernstein et al., 2017; Pucci et al., 2020).

To improve accuracy and standardization, Patient-Specific Templates (PSTs) have been introduced as custom-made surgical guides derived from preoperative imaging data. PSTs provide rigid mechanical guidance to the cutting instrument and have demonstrated improved precision compared to free-hand techniques (García y Sánchez et al., 2015; Picón et al., 2021; Liu et al., 2024). However, their effectiveness relies on accurate fitting to the patient's bone surface, which may be compromised by anatomical changes or limited surgical exposure (Caiti et al., 2018; Aiba et al., 2023). In addition, PSTs typically require large contact surfaces, are invasive, and are designed for single-use applications, limiting their flexibility and increasing costs (Lin et al., 2015; Hess et al., 2024).

Augmented Reality (AR) has emerged as an alternative approach by allowing virtual visualization of anatomical structures and planned cutting planes directly in the surgical field (Gao et al., 2019; Zhao et al., 2023; Ulrich et al., 2024). AR-based guidance enhances intraoperative visualization and enables dynamic adjustment of the surgical plan without the need for physical guides. Nevertheless, AR-only solutions lack rigid mechanical constraints, making the accuracy of the osteotomy highly dependent on the surgeon's ability to follow virtual cues, which

* Corresponding author.
E-mail address: federico.salerno@polito.it (F. Salerno).

https://doi.org/10.1016/j.jcms.2026.104480
Received 5 November 2025; Accepted 24 January 2026
Available online 19 February 2026

Table 1
Comparison of representative approaches for mandibular osteotomy guidance. FH: free-hand technique; PST: patient-specific template; AR: augmented reality. Reported outcomes refer to the deviation between planned and achieved osteotomy planes or anatomical positioning, as provided by the respective authors.

Reference	Approach	Application	Validation	Reported outcome
Ferri et al. (1997)	FH	Mandibular reconstruction	Clinical	2-4 mm deviation
Smatt and Ferri (2005)	FH	Maxillomandibular advancement	Clinical	3-5 mm deviation
De Maesschalck et al. (2017)	PST	ORN mandibular resection	Clinical	~2 mm deviation
Picón et al. (2021)	PST	Mandibular reconstruction	Phantom	1-2 mm deviation
Kim et al. (2020)	PST	Mandibular reconstruction	Clinical	1.5 mm (PST) vs 4 mm (free-hand)
Zhu et al. (2017)	AR	Nerve bundle visualization	Phantom	0.96 ± 0.51 mm error
Sahovaler et al. (2021)	AR	Sinonasal tumor resection	Clinical	Intratumoral cuts reduced to 9.4%
Lin et al. (2022)	AR	Craniofacial fracture reduction	Phantom	1.35 mm placement error
Battaglia et al. (2019)	AR + PST	Fibular free flap harvesting	Phantom	<2 mm alignment deviation
Moreta-Martinez et al. (2020)	AR + PST	Orthopedic oncology	Phantom	~2 mm placement accuracy
Moreta-Martinez et al. (2021)	AR + PST	Orthopedic oncology	Clinical	~2 mm placement accuracy
Mendicino et al. (2022)	AR + PST	Resection planning	Phantom	2.19 mm positioning error

may introduce variability and reduce precision (Meulstee et al., 2019; Pietruski et al., 2019; Vles et al., 2020).

To combine the advantages of both approaches, hybrid solutions integrating PSTs with AR guidance have been proposed. In these systems, AR supports the positioning and verification of the physical guide, while the PST ensures precise execution of the osteotomy (Moreta-Martinez et al., 2020; Mendicino et al., 2022; Ceccariglia et al., 2022). Despite these improvements, existing hybrid approaches often remain limited by rigid anchoring mechanisms and low adaptability to different surgical scenarios.

In this work, we propose a hybrid physical-AR surgical cutting guide designed to improve flexibility while preserving mechanical accuracy. The system combines a generalized anchoring mechanism with an adjustable cutting plane and AR-based guidance implemented through an inside-out tracking approach. The proposed solution is validated on a 3D-printed anatomical mockup under simulated surgical conditions, with the aim of assessing its feasibility and potential clinical applicability.

The present paper is organized as follows: Section 2 provides an analysis of related works. Section 3 describes the physical device, along with the AR guidance system, followed by the evaluation metrics and the experimental setup. The results are presented in Section 4, while Section 5 includes a critical analysis of the results and a comparison with values reported in the literature. Finally, Section 6 summarizes the conclusions.

2. Related works

Several approaches have been proposed in the literature to support mandibular osteotomies with the aim of improving accuracy, reproducibility, and intraoperative control. Early studies primarily relied on free-hand techniques, which offer procedural flexibility but show limited reproducibility and accuracy in complex reconstructions.

To address these limitations, Patient-Specific Templates (PST) were introduced to provide rigid, anatomy-driven guidance, significantly improving cutting precision. However, their dependence on accurate bone fitting and limited adaptability restrict their use in dynamic surgical scenarios.

More recently, Augmented Reality (AR) has been investigated as a means to provide real-time visualization of anatomical structures and planned cutting planes, improving intraoperative awareness while lacking physical constraints on the cutting tool. Hybrid AR-PST approaches attempt to combine the complementary advantages of both strategies, enabling guided placement and verification of physical cutting guides.

To improve clarity and conciseness, representative studies are summarized and compared in Table 1, highlighting the main methodological differences, application contexts, and reported outcomes.

3. Materials and methods

This section describes the operational workflow for the application of the hybrid device on the patient and provides the design details of the physical component and the AR guidance system. More specifically, the following subsections detail the operational workflow for the use of the hybrid system by surgical personnel, the design details of the physical component, the AR guidance procedure, the evaluation metrics employed to assess its performance, and the experimental setup used to validate the system in an *in vitro* scenario.

3.1. Physical device

From an analysis of the state-of-the-art on surgical guide (SG) design characteristics, three fundamental features common to all SGs were identified: (1) stable placement on a specific portion of the mandibular bone, (2) the use of a fixation screw to ensure stability. (3) a slot to guide the surgical blade during osteotomy.

Building on these foundational features, we propose an SG design that can be positioned on a generic mandibular surface, offering adjustability in the position and orientation of the cutting plane. Specifically, the proposed guide incorporates the following: (*i*) Adaptability to a generic surface: the guide does not require anatomical fitting for installation. Instead, it employs three support pins of adjustable height, designed to prevent interference with the rest of the structure, enabling placement on diverse mandibular surfaces. (*ii*) Stable fixation to the bone: a single fixation screw anchors the guide to the bone tissue. The screw is tightened only after determining the optimal position, ensuring secure attachment. (*iii*) Rigid support for the cutting blade: a slot, matching the thickness of the surgical blade, provides a rigid guide for the blade during osteotomy. The slot is oriented to align with the target cutting plane as defined in the surgical plan. (*iv*) Adjustability of the cutting plane support: the rigid blade support is connected to the anchoring system via a mechanism that allows relative movement between the two components. This adjustability enables precise alignment with the target cutting plane.

Fig. 1 illustrates ten state-of-the-art mandibular surgical guides in the upper section. The middle section highlights the basic features identified through an analysis of their design characteristics. The lower section presents the features of the surgical guide proposed in this study.

3.2. CAD design and structural details

The SG consists of key components: an anchoring support, adjustment screws, an adjustable blade plane, and a tracked marker. The anchoring support adapts to various surfaces using three adjustable

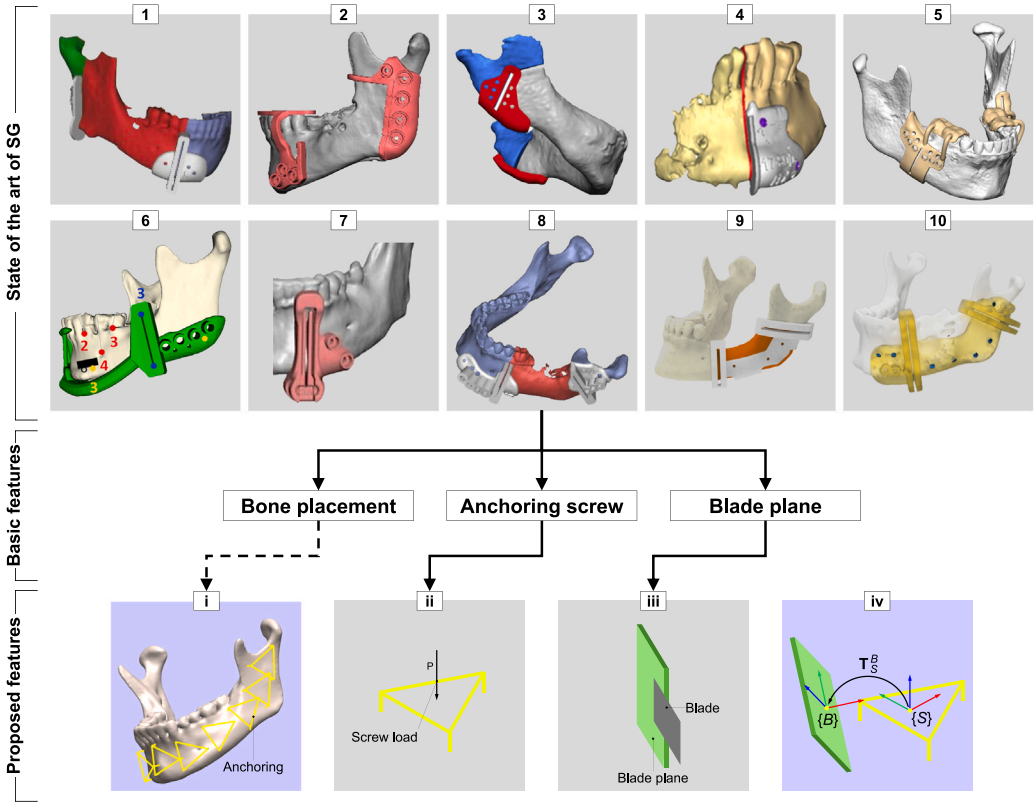

Fig. 1. Features of the proposed surgical guide derived from the state-of-the-art. Top: examples of state-of-the-art surgical guides: (1) (Wang et al., 2016), (2) (Franco and Farrell, 2016), (3) (Resnick, 2018), (4) (Blanc et al., 2019), (5) (Badiali et al., 2020), (6) (Brouwer de Koning et al., 2021), (7) (Myers et al., 2021), (8) (Massarelli and Meloni, 2022), (9) (Xilloc, 2025), and (10) (Customy, 2025). Middle: the extracted basic features of these guides. Bottom: the proposed features derived from the basic ones, including (*i*) placement on a generic portion of the mandible, (*ii*) stable fixation with a screw, (*iii*) a blade plane for the cutting blade, and (*iv*) a novel feature i.e. the adjustability of the blade plane.

conical supports. It includes threaded holes for screw fixation. Adjustment screws allow precise positioning of the guide. A fixation screw anchors the guide to the bone after the optimal position is confirmed. The blade plane holds the surgical blade in place, aligned with the target cutting plane. The blade plane moves smoothly, guided by spherical joints and adjustment screws. These joints allow the blade plane to translate or rotate, depending on screw adjustments. The blade plane integrates a marker system for AR tracking. The marker system and blade plane form a rigid body for precise position tracking. The system continuously adjusts the blade plane to align with the target cutting plane. An ArUco marker (30 mm) is used for pose estimation (Garrido-Jurado et al., 2014). Fig. 2 shows the proposed guide, highlighting its components and application for guided osteotomy.

Parts were designed using SolidWorks CAD and fabricated with a Prusa MK3S 3D printer using PLA filament.

3.3. Augmented module

The AR guidance is designed to facilitate the adjustment of the blade plane in accordance with target planes. It acts as a visual guiding support, displayed through the HMD Hololens 2, to assist in regulating the surgical guide after it has been applied to the patient.

3.3.1. Hologram registration

A registration procedure is performed to align the physical mockup with its virtual representation. A 3D-printed mannequin including a face and mandible is used to simulate patient anatomy. Predefined cephalometric landmarks are digitized using a tracked tool, providing repeatable and operator-independent registration (Salerno et al., 2026). The virtual model includes corresponding anatomical structures, landmarks, and planned cutting planes, which are aligned to the physical model through landmark digitization. The tracked tool is localized in real time using marker-based tracking detected by the AR device cameras, enabling accurate digitization of physical landmarks within a common reference frame. Marker detection and pose estimation are performed automatically using standard computer vision routines (Salerno et al., 2025), enabling robust localization of the tool tip. A robust vision-based approach is used to estimate the tool pose, ensuring reliable landmark digitization despite noise and minor occlusions. The overall registration workflow, including the spatial relationships and transformations involved in the digitization and alignment process, is schematically illustrated in Fig. 3.

The physical and virtual landmark sets are aligned by computing a rigid transformation that minimizes their spatial discrepancy, resulting in an accurate overlay of the virtual anatomical model onto the physical mockup.

3.3.2. Augmented reality guidance

After registration, the application provides two main user flows on HoloLens 2: an on-device *tutorial* and an *operative procedure* supporting the surgical workflow. The tutorial (Fig. 4) introduces the surgical context, the AR visualized assets (face and mandible models, cutting planes), and the expected user interactions. It also provides an overview of the two feedback modes available during the procedure: *F1*, based on visual plane overlay, and *F2*, based on proximity guidance. This briefing clarifies the inputs, displayed information, and sequence of tasks before the operative phase.

The operative procedure (Fig. 5) starts with subject selection and point-based registration of the anatomical part. During registration,

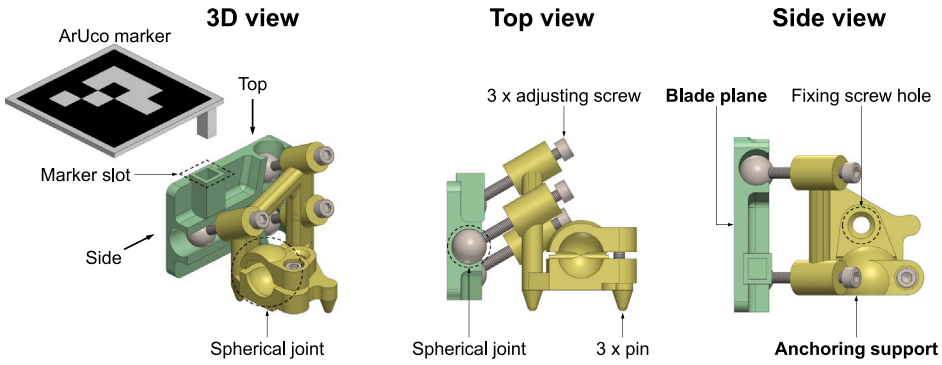

Fig. 2. Constructive and functional details of the cutting guide: (a) Exploded view of the guide; (b) Assembled cutting guide without the ArUco marker; (c) Rotation axes of the blade plane (red) and screw adjustment axes (blue); (d) Cutting guide mounted on the mandible aligned with the target plane (purple), including an example of a handpiece with a surgical blade for guided osteotomy.

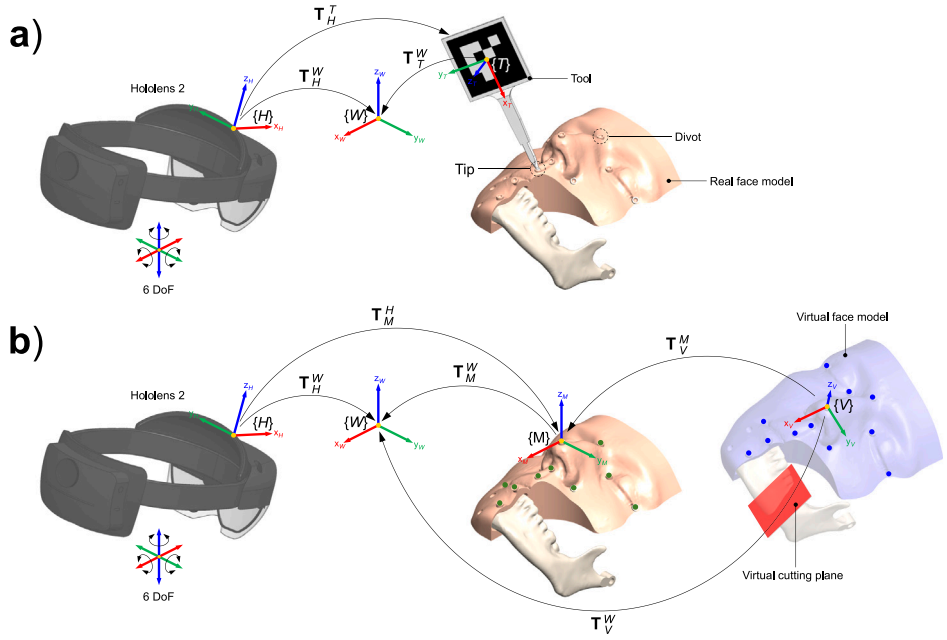

Fig. 3. Registration of the virtual anatomical model onto the 3D mockup: (a) Digitization of cephalometric landmarks using the tracked tool; (b) Overlay of the virtual model through point cloud alignment.

alignment quality is quantified through the RMSD distance. After registration, virtual models of the face and mandible and the target cutting planes are overlaid onto the physical mock-up or patient anatomy. A marker rigidly attached to the blade plane is continuously tracked to update its pose. The operator selects the feedback mode: F1 supports visual alignment through holographic plane overlay, while F2 provides additional proximity guidance through graphical cues and numerical distance readouts. Fig. 5 illustrates the procedure flow and the proximity feedback associated with F2. Throughout the procedure, visualization, plane selection, and measurement readouts remain co-located within the AR view to support intraoperative interaction.

The application was developed in Unity 2022.3.28f1 for interface layout and scene management, with anatomical models designed in Blender 3.5.0 and deployed on HoloLens 2 using Visual Studio 2022.

MRTK 3 was integrated to support mixed-reality interaction, while the OpenCV plugin for Unity enabled marker-based tracking and pose estimation.

3.4. Evaluation metrics

To evaluate the accuracy of the AR-guided blade plane adjustment, the protruding length of each screw shaft was measured for the three target osteotomy plane positions and compared with the expected values from the CAD model.

Specific reference seats were designed on the mandible to ensure repeatable positioning of the guide.

Protruding screw lengths derived from the CAD model were used as ground truth.

The screw positioning errors were computed as:

$$E1 = l_1 - \tilde{l}_1, \quad E2 = l_2 - \tilde{l}_2, \quad E3 = l_3 - \tilde{l}_3, \tag{1}$$

To evaluate blade plane orientation with respect to the target plane, the angle α between the corresponding normal vectors was computed for each target position.

In addition, the distance d between the points of application of the normal vectors was measured (Fig. 6).

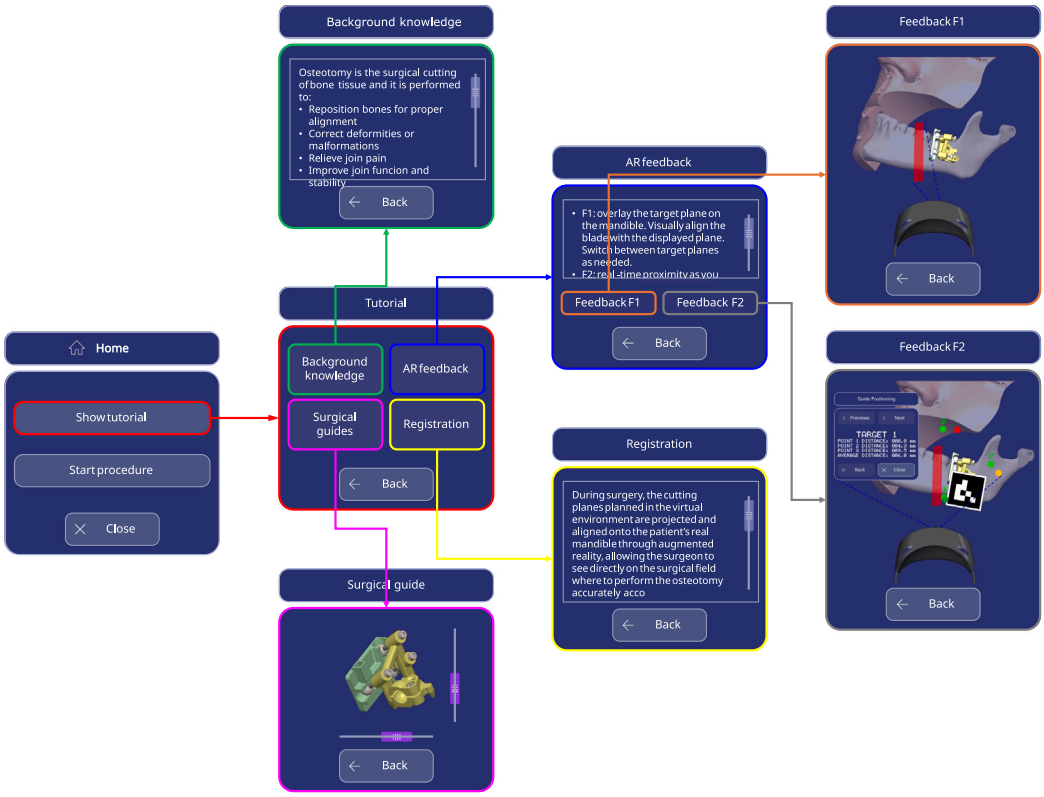

Fig. 4. Tutorial: overview of context, AR assets, and preview of the two feedback modes (F1 and F2).

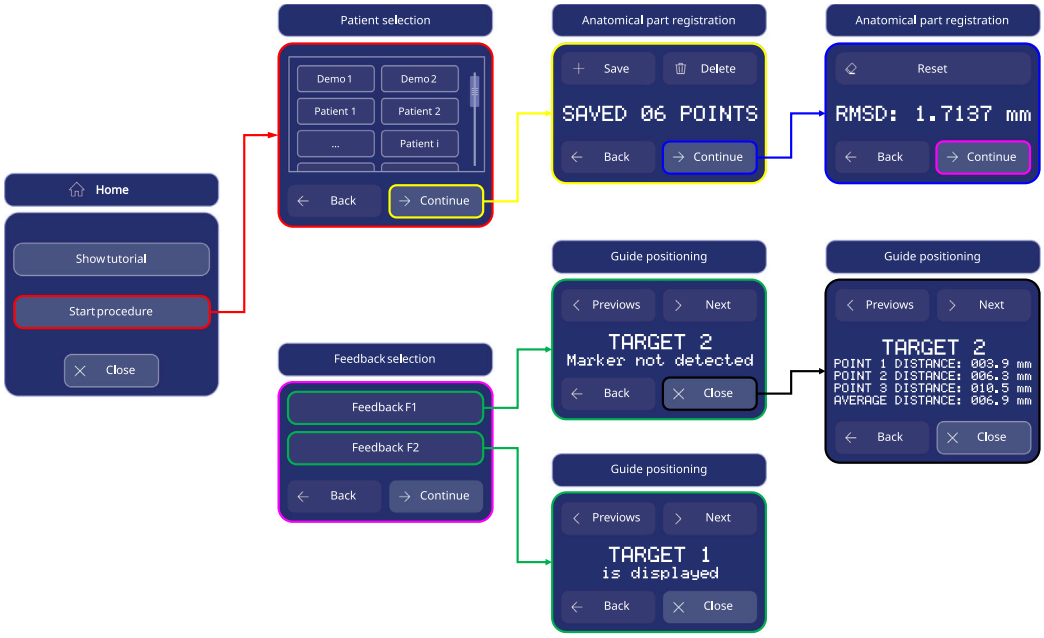

Fig. 5. Operative procedure: subject selection, registration with distance metrics, feedback mode selection (F1/F2), and detail of the F2 proximity windows; F1 provides holographic plane navigation.

The registration accuracy was quantified by computing the Root Mean Square Deviation (RMSD) across the 14 cephalometric landmarks:

$$\mathrm{RMSD} = \sqrt{\frac{1}{N}\sum_{i=1}^{N}\left(\mathbf{v}^{W} - \mathbf{v}_{T}^{W}\right)^{2}} \tag{2}$$

3.5. Experimental setup

The experiment evaluated the ability to adjust the cutting guide to predefined target planes under different feedback conditions. In each trial, the operator aligned the guide by adjusting three screws until the target position was reached. Three independent factors were

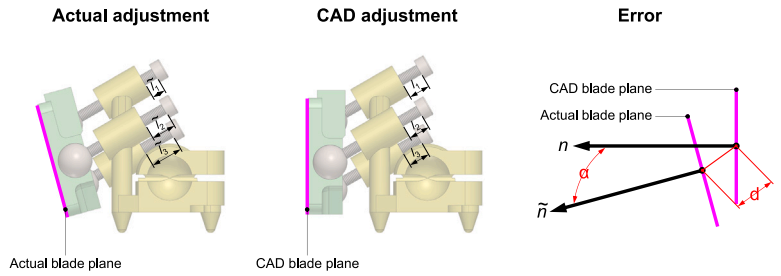

Fig. 6. Schematic representation of the evaluation metrics: angle α and distance d between the actual cutting plane and the planned target plane.

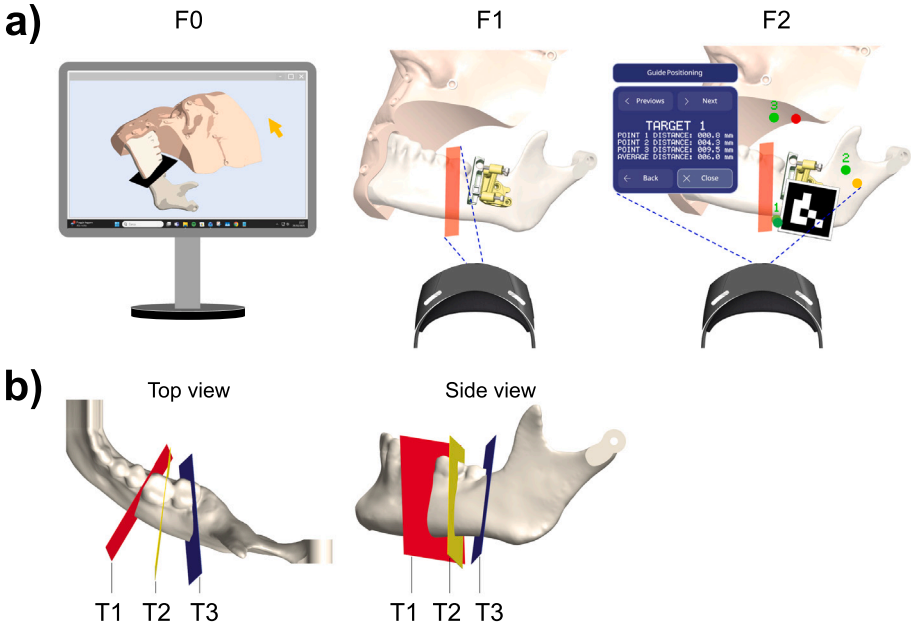

Fig. 7. Overview of experimental conditions for surgical guide adjustment: (a) feedback modalities, from left to right: F0, monitor-based visualization showing the 3D model of the target cutting plane; F1, augmented reality overlay of the target plane onto the 3D-printed mandibular mock-up using HoloLens 2; F2, AR-based guidance combining three complementary mechanisms, namely (i) twin holographic sphere sets, one associated with the target plane and one rigidly attached to the blade plane, enabling immediate visual alignment, (ii) a red-to-green color transition of the blade-plane spheres as they approach the target positions, and (iii) numerical readouts of the Euclidean distances between corresponding sphere centers to quantify alignment accuracy; (b) predefined target cutting planes T1, T2, and T3, each requiring an independent adjustment.

considered: operator experience, feedback modality, and target plane. Two expert (E) and two non-expert (NE) participants performed the task. All participants were affiliated with the Maxillofacial Surgery Unit of the Department of Surgical Sciences, Città della Salute e della Scienza di Torino, Molinette University Hospital (Turin, Italy). The expert group included two cranio-maxillofacial surgeons, while the non-expert group consisted of two residents in maxillofacial surgery. Three feedback modalities were tested: F0, based on a standard monitor displaying the target plane; F1, providing AR overlay of the target plane on the mock-up via HoloLens 2; and F2, extending F1 with real-time graphical and numerical proximity feedback (Fig. 7a).

Three predefined target planes (T1, T2, T3) were defined, each requiring an independent adjustment (Fig. 7b). Each experimental session consisted of multiple trials, with the sequence of target planes randomized for each participant to minimize order effects. For AR-based feedback (F1 and F2), a single registration was performed per feedback condition and reused across all target planes. The registration was maintained while adjusting all target planes within the same feedback condition, following the randomized order. Each operator completed all feedback and target plane combinations, with each condition repeated five times.

4. Results

4.1. Descriptive overview

Table 2 reports descriptive statistics for screw length errors (E1, E2, E3), the distance d between the achieved and target cutting planes, and the angular deviation α, for the three feedback conditions (F0–F2). Across conditions, plane misalignment decreased when AR feedback was available: the highest mean d was observed in F0 (2.15 mm), while the lowest mean d was observed in F2 (1.27 mm). Similarly, α was highest in F0 (7.71°), whereas lower mean values were obtained with AR (4.16° in F1 and 4.46° in F2). Screw errors showed condition-dependent variability, with the largest dispersion observed for E3 in F0 ($s = 3.19$ mm).

A distribution fitting procedure (Razali et al., 2011) was performed to assess normality prior to inferential statistics. E1–E3 were approximately normally distributed, whereas d and α showed non-normal behavior; therefore, parametric analyses were applied to E1–E3, while non-parametric tests were used for d and α. In addition, Grubbs' test (Grubbs, 1949) did not identify significant outliers in E1–E3 at $\alpha = 0.05$, and all measurements were retained for subsequent analyses.

Table 2
Summary statistics for E1, E2, E3, d, and α variables. V: variable, m: mean, s: standard deviation, min: minimum value, $Q1$: first quartile, M: median, $Q3$: third quartile, max: maximum value.

	V	m	s	min	$Q1$	M	$Q3$	max
F0	E1/mm	0.88	2.79	−6.61	−1.18	0.02	3.63	6.99
	E2/mm	0.66	1.47	−1.80	−0.53	0.51	1.60	3.61
	E3/mm	0.28	3.19	−6.99	−2.44	0.92	3.08	6.19
	d/mm	2.15	1.01	0.73	1.21	1.90	2.86	4.69
	α/°	7.71	3.81	1.18	4.67	7.23	10.04	16.15
F1	E1/mm	0.66	1.62	−1.91	−0.41	0.37	1.27	6.28
	E2/mm	0.69	1.33	−1.48	−0.38	0.56	1.44	3.95
	E3/mm	1.03	1.54	−1.57	−0.05	0.59	2.02	5.05
	d/mm	1.48	1.19	0.32	0.59	1.10	1.75	5.48
	α/°	4.16	2.93	0.48	2.12	3.70	5.32	16.03
F2	E1/mm	−0.25	1.77	−5.55	−0.99	−0.45	0.58	5.29
	E2/mm	−0.66	1.22	−3.68	−1.41	−0.75	−0.14	2.28
	E3/mm	−0.04	1.26	−2.59	−0.83	−0.37	0.76	3.72
	d/mm	1.27	0.71	0.37	0.79	1.13	1.55	3.53
	α/°	4.46	3.27	0.31	2.14	4.09	5.52	19.47

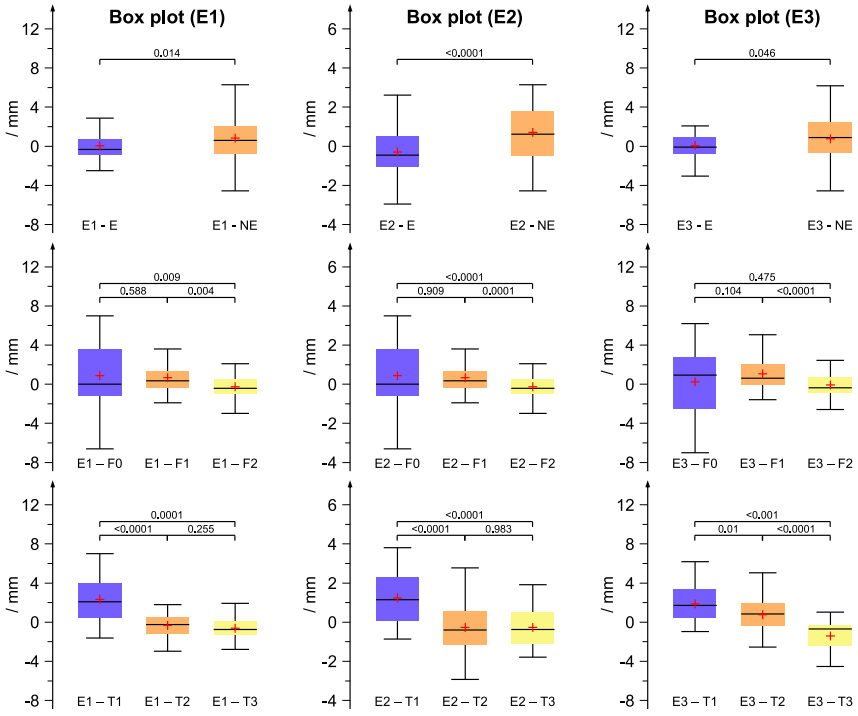

Fig. 8. Box plots showing the effects of *Operator*, *Feedback*, and *Target* on E1, E2, and E3.

4.2. Effects on screw errors (E1–E3)

A three-way ANOVA was conducted to evaluate the effects of *Feedback* (F0–F2), *Operator* (E vs. NE), and *Target* (T1–T3) on E1, E2, and E3. For E1 and E2, *Feedback* had a significant effect (E1: $p < 0.001$; E2: $p < 0.0001$), with F2 yielding lower errors than F0 and F1; no significant difference was observed between F0 and F1. *Operator* was significant for E1–E3 (E1: $p = 0.001$; E2: $p < 0.0001$; E3: $p = 0.009$), with non-expert participants showing larger errors overall. *Target* had the strongest influence on all screw-error variables ($p < 0.0001$), with T1 associated with the highest errors; T3 showed the lowest values, particularly for E3.

Post-hoc comparisons (Bonferroni-corrected) confirmed that the main differences were driven by (i) lower errors in F2 compared with F0/F1 for E1 and E2, and (ii) consistently higher errors for non-experts compared with experts. Fig. 8 summarizes the distribution of E1–E3 across the experimental factors.

4.3. Effects on plane misalignment (d and α)

The effects of *Operator*, *Feedback*, and *Target* on d and α were assessed using Kruskal–Wallis tests with Dunn's post-hoc comparisons. *Operator* significantly affected both d ($p < 0.0001$) and α ($p < 0.0001$), with non-experts showing larger misalignment. *Feedback* also significantly affected both metrics ($p < 0.0001$), with F0 producing higher d and α than the AR-based conditions (F1 and F2). No significant difference was observed between F1 and F2 for either d ($p = 0.814$) or α ($p = 0.631$). In contrast, *Target* did not show a significant effect on d ($p = 0.137$) or α ($p = 0.078$). Fig. 9 reports the distributions of d and α across factors.

Fig. 10 reports the registration accuracy expressed as RMSD across the cephalometric landmarks used to align the virtual model to the physical mock-up.

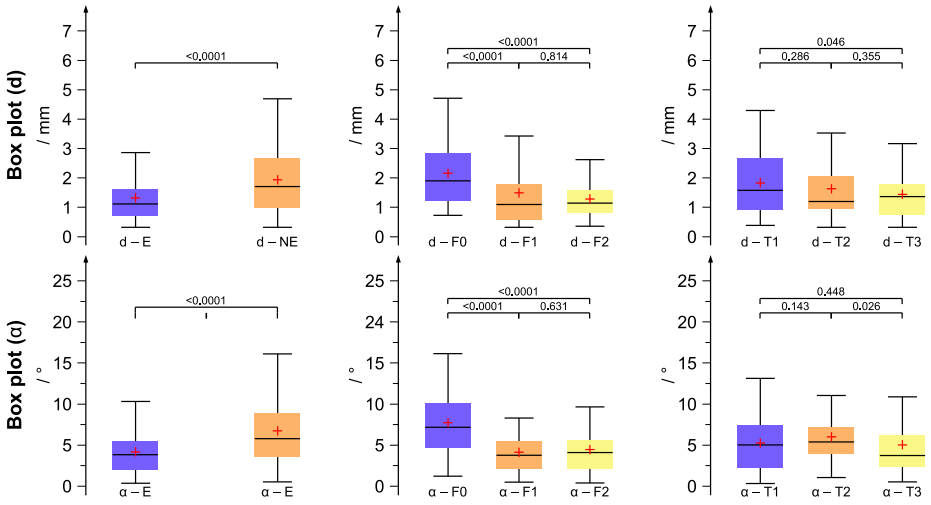

Fig. 9. Box plots depicting the effects of *Operator*, *Feedback*, and *Target* on d (top) and α (bottom).

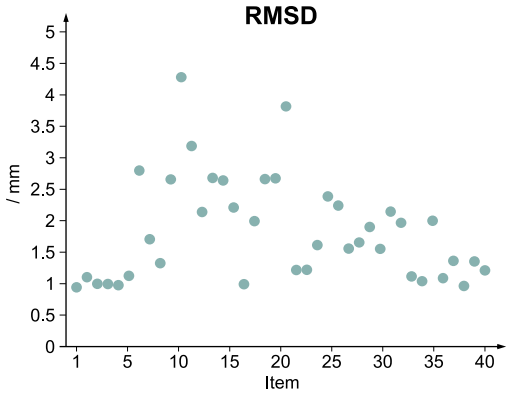

Fig. 10. Registration accuracy expressed as RMSD across the cephalometric landmarks used for alignment.

5. Discussion

This study investigated the feasibility of an adjustable cutting guide system for osteotomies, integrating augmented reality (AR) to assist in plane alignment. The proposed system allows intraoperative adjustment of the blade plane through the rotation of three screws, enabling adaptation to different target planes. Unlike conventional tracking methods that rely on external markers, the AR-based registration in this study follows an inside-out approach, reducing system complexity and improving ease of use. The system was evaluated in a controlled experiment, where expert and non-expert operators adjusted the cutting guide to match three predefined target planes under different feedback conditions.

As reported by Smatt and Ferri (2005), free-hand mandibular advancement procedures resulted in positional deviations of 10.66 ± 2.82 mm and angular deviations of 5.48 ± 1.4°. Compared to our results, particularly under *Feedback-0*, which yielded 2.15 ± 1.01 mm and 7.71 ± 3.81°, our method exhibited a substantially lower positional error but a slightly higher angular deviation. The introduction of AR guidance further improved positional accuracy, with deviations decreasing to 1.27 ± 0.71 mm in *Feedback-2*, reinforcing the potential of AR-assisted adjustments in achieving greater precision.

Kim et al. (2020) reported surgical guide deviations ranging from 0.85 mm to 2.56 mm, comparable to our results with *Feedback-2* (1.27 ± 0.71 mm) and *Feedback-1* (1.48 ± 1.19 mm). However, without AR guidance *Feedback-0*, our deviation increased to 2.15 ± 1.01 mm, exceeding their reported range. The study by De Maesschalck et al. (2017) compared CAS with a traditional freehand technique in mandibular reconstruction. Their results showed a mean distance deviation of 2.3 ± 1.0 mm for mandibular osteotomies and 1.9 ± 1.1 mm for fibular osteotomies. These values are comparable to our results, particularly under *Feedback-1* (1.48 ± 1.19 mm) and *Feedback-2* (1.27 ± 0.71 mm).

In the study by Gao et al. (2019), an augmented reality-based deviation-reminder system was evaluated for mandibular angle split osteotomy. Their results showed a mean positional error of 1.89 ± 0.51 mm for surgeons using the AR guidance, while the orientation error was 2.03 ± 1.15°. These values are comparable to our results with *Feedback-2*, where we observed slightly better positional accuracy 1.27 ± 0.71 mm and a higher angular error of 4.46 ± 3.27°.

Mendicino et al. (2022) investigated the use of augmented reality to guide patient-specific template placement in pelvic resections. Their system achieved a mean placement error of 2.19 ± 1.23 mm, demonstrating an improvement over conventional PST methods. In comparison, our results showed a mean deviation of 1.27 ± 0.71 mm with *Feedback-2*, indicating that dynamic feedback can further enhance positioning accuracy.

The present study evaluated the accuracy of aligning a cutting guide to a predefined target plane but did not assess the actual osteotomy outcome. This represents a limitation, as deviations in tool handling and intraoperative factors may influence the final cut beyond the initial guide alignment. Additionally, the registration process relied on divots as fiducial markers, which ensured consistent and accurate landmark localization by constraining the registration tool to predefined locations, thereby minimizing localization errors. Another limitation concerns the experimental setup, which was conducted on a rigid 3D-printed mandibular mockup rather than a model incorporating soft tissue. The absence of soft tissue eliminated potential deformations during the digitization process of the registration, which could otherwise introduce inaccuracies in a clinical scenario.

Future work should explore the application of the adjustable cutting guide in different anatomical regions of the mandible and on various bone structures to assess its versatility and adaptability. Furthermore, an important next step is to evaluate the accuracy of the actual osteotomy by performing cuts and measuring deviations between the planned and executed cutting planes. This would provide a more comprehensive validation of the system's clinical feasibility and precision.

6. Conclusions

This study presented a hybrid surgical guide that integrates a physical anchoring system with adjustable geometry and augmented reality feedback for intraoperative alignment. The proposed design departs from conventional patient-specific templates by introducing adaptability to generic bone surfaces and the possibility of adjusting the cutting plane intraoperatively. The experimental evaluation on 3D-printed mandibular phantoms showed that augmented reality feedback significantly improved the accuracy of guide adjustment compared to conditions without virtual assistance. Positional deviations were reduced to values comparable with those reported in the literature for patient-specific templates, while maintaining a flexible and reusable design. The analysis also highlighted the influence of operator experience, with experts consistently achieving smaller errors than non-experts, and confirmed that enhanced feedback modalities can mitigate part of this variability. The results demonstrate the feasibility of combining physical and digital paradigms to achieve a more adaptable form of osteotomy guidance. While the validation was limited to phantom experiments and alignment accuracy, further studies should investigate the translation of this system to actual osteotomy execution, the integration of soft-tissue models, and the evaluation of clinical usability.

CRediT authorship contribution statement

Federico Salerno: Conceptualized the work, Developed the methodology, Implemented the software, Performed the validation, Conducted the formal analysis and investigation, Curated the data, Handled the visualizations, Wrote the original draft. **Luca Ulrich:** Conceptualization, Methodology, Software development, Validation, Formal analysis, Visualization, Original draft writing. **Giorgia Marullo:** Performed formal analysis and validation, Supervised the work, Contributed to review and editing. **Sandro Moos:** Conceptualization, Supervision, Funding acquisition, Review and editing. **Enrico Vezzetti:** Supervision, Project administration, Funding acquisition, Contributed to review and editing.

Funding

This work was funded by the DAS — Design for Augmented Surgery project, developed within the framework of the "BANDO AGGREGAZIONI R&S – SALUTE" call. The project was co-financed by the European Regional Development Fund (ERDF) under the Valle d'Aosta Regional Programme 2021–2027.

Declaration of competing interest

The authors declare that they have no known competing financial interests or personal relationships that could have appeared to influence the work reported in this paper.

Acknowledgments

The authors would like to express their sincere gratitude to Prof. Guglielmo Ramieri and the staff of the Cranio-Maxillofacial Surgery Department at the "Città della Salute e della Scienza di Torino" (Molinette Hospital, Turin, Italy) for their valuable clinical insights and support during the development of this work. All authors reviewed and approved the final manuscript.

Data availability

Data sets generated during the current study are available from the corresponding author on reasonable request.

References

Aiba, H., Spazzoli, B., Tsukamoto, S., Mavrogenis, A.F., Hermann, T., Kimura, H., Murakami, H., Donati, D.M., Errani, C., 2023. Current concepts in the resection of bone tumors using a patient-specific three-dimensional printed cutting guide. Curr. Oncol. 30, 3859–3870. http://dx.doi.org/10.3390/curroncol30040292.

Badiali, G., Bevini, M., Ruggiero, F., Cercenelli, L., Lovero, E., De Simone, E., Rucci, P., Bianchi, A., Marchetti, C., 2020. Validation of a patient-specific system for mandible-first bimaxillary surgery: Ramus and implant positioning precision assessment and guide design comparison. Sci. Rep. 10, 13317. http://dx.doi.org/10.1038/s41598-020-70107-w.

Battaglia, S., Badiali, G., Cercenelli, L., Bortolani, B., Marcelli, E., Cipriani, R., Contedini, F., Marchetti, C., Tarsitano, A., 2019. Combination of cad/cam and augmented reality in free fibula bone harvest. Plast. Reconstr. Surg. 7, e2510. http://dx.doi.org/10.1097/GOX.0000000000002510.

Bernstein, J.M., Daly, M.J., Chan, H., Qiu, J., Goldstein, D., Muhanna, N., de Almeida, J.R., Irish, J.C., 2017. Accuracy and reproducibility of virtual cutting guides and 3d-navigation for osteotomies of the mandible and maxilla. PLoS One 12, e0173111. http://dx.doi.org/10.1371/journal.pone.0173111.

Blanc, J., Fuchsmann, C., Nistiriuc-Muntean, V., Jacquenot, P., Philouze, P., Ceruse, P., 2019. Evaluation of virtual surgical planning systems and customized devices in fibula free flap mandibular reconstruction. Eur. Arch. Otorhinolaryngol. 276, 3477–3486. http://dx.doi.org/10.1007/s00405-019-05625-z.

Caiti, G., Dobbe, J.G., Strijkers, G.J., Strackee, S.D., Streekstra, G.J., 2018. Positioning error of custom 3d-printed surgical guides for the radius: influence of fitting location and guide design. Int. J. Comput. Assist. Radiol. Surg. 13, 507–518. http://dx.doi.org/10.1007/s11548-017-1682-6.

Ceccariglia, F., Cercenelli, L., Badiali, G., Marcelli, E., Tarsitano, A., 2022. Application of augmented reality to maxillary resections: A three-dimensional approach to maxillofacial oncologic surgery. J. Pers. Med. 12, 2047. http://dx.doi.org/10.3390/jpm12122047.

Chang, Y.M., Chana, J.S., Wei, F.C., Tsai, C.Y., Chen, S.H., 2003. Osteotomy to treat malocclusion following reconstruction of the mandible with the free fibula flap. Springer Spec. Surg. S 112, 31–36. http://dx.doi.org/10.1097/01.PRS.0000065910.66161.DD.

Customy, 2025. Custom surgical guides - craniofacial solutions. https://customy.eu/craniofacial/custom-surgical-guides/. (Accessed 13 January 2025).

De Maesschalck, T., Courvoisier, D.S., Scolozzi, P., 2017. Computer-assisted versus traditional freehand technique in fibular free flap mandibular reconstruction: a morphological comparative study. Eur. Arch. Otorhinolaryngol. 274, 517–526. http://dx.doi.org/10.1007/s00405-016-4246-4.

Ferri, J., Piot, B., Ruhin, B., Mercier, J., 1997. Advantages and limitations of the fibula free flap in mandibular reconstruction. J. Oral Maxil. Surg. 55, 440–448. http://dx.doi.org/10.1016/S0278-2391(97)90685-6.

Franco, P.B., Farrell, B.B., 2016. Inverted l osteotomy: a new approach via intraoral access through the advances of virtual surgical planning and custom fixation. Oral Maxillofac. Surg. Cases 2, 1–9. http://dx.doi.org/10.1016/j.omsc.2016.01.001.

Gao, Y., Lin, L., Chai, G., Xie, L., 2019. A feasibility study of a new method to enhance the augmented reality navigation effect in mandibular angle split osteotomy. J. Craniomaxillofac. Surg. 47, 1242–1248. http://dx.doi.org/10.1016/j.jcms.2019.04.005.

Garrido-Jurado, S., Muñoz-Salinas, R., Madrid-Cuevas, F.J., Marín-Jiménez, M.J., 2014. Automatic generation and detection of highly reliable fiducial markers under occlusion. Pattern Recognit. 47, 2280–2292. http://dx.doi.org/10.1016/j.patcog.2014.01.005.

Grubbs, F.E., 1949. Sample Criteria for Testing Outlying Observations. University of Michigan, http://dx.doi.org/10.1214/aoms/1177729885.

Hess, S., Husarek, J., Müller, M., Eberlein, S.C., Klenke, F.M., Hecker, A., 2024. Applications and accuracy of 3d-printed surgical guides in traumatology and orthopaedic surgery: A systematic review and meta-analysis. J. Exp. Orthop. 11, e12096. http://dx.doi.org/10.1002/jeo2.12096.

Kim, S.R., Jang, S., Ahn, K.M., Lee, J.H., 2020. Evaluation of effective condyle positioning assisted by 3d surgical guide in mandibular reconstruction using osteocutaneous free flap. Materials 13, 2333. http://dx.doi.org/10.3390/ma13102333.

Kommers, S.C., Van Den Bergh, B., Boffano, P., Verweij, K.P., Forouzanfar, T., 2014. Dysocclusion after maxillofacial trauma: a 42 year analysis. J. Craniomaxillofac. Surg. 42, 1083–1086. http://dx.doi.org/10.1016/j.jcms.2013.05.013.

Brouwer de Koning, S., Geldof, F., van Veen, R., van Alphen, M., Karssemakers, L., Nijkamp, J., Schreuder, W., Ruers, T., Karakullukcu, M., 2021. Electromagnetic surgical navigation in patients undergoing mandibular surgery. Sci. Rep. 11, 4657. http://dx.doi.org/10.1038/s41598-021-84129-5.

Lin, H.H., Chang, H.W., Lo, L.J., 2015. Development of customized positioning guides using computer-aided design and manufacturing technology for orthognathic surgery. Int. J. Comput. Assist. Radiol. Surg. 10, 2021–2033. http://dx.doi.org/10.1007/s11548-015-1223-0.

Lin, L., Gao, Y., Aung, Z.M., Xu, H., Wang, B., Yang, X., Chai, G., Xie, L., 2022. Preliminary reports of augmented-reality assisted craniofacial bone fracture reduction. J. Plast. Reconstr. Aesthetic Surg. 75, e1–e8. http://dx.doi.org/10.1016/j.bjps.2022.06.105.

Liu, Z., Zhong, Y., Lyu, X., Zhang, J., Huang, M., Liu, S., Zheng, L., 2024. Accuracy of the modified tooth-supported 3d printing surgical guides based on ct, cbct, and intraoral scanning in maxillofacial region: A comparison study. J. Stomatol. Oral Maxillofac. Surg. 101853. http://dx.doi.org/10.1016/j.jormas.2024.101853.

Massarelli, O., Meloni, S.M., 2022. The "beveled one-and-a-half-barrel" fibula transplant with virtual surgical planning and ct-guided implant surgery for prosthetic rehabilitation in posterior mandible defects: A pictorial essay. J. Diagn. Treat Oral Maxillofac. Pathol. 6, 39–59. http://dx.doi.org/10.23999/j.dtomp.2022.3.3.

Mendicino, A.R., Condino, S., Carbone, M., Cutolo, F., Cattari, N., Andreani, L., Parchi, P.D., Capanna, R., Ferrari, V., 2022. Augmented reality as a tool to guide patient-specific templates placement in pelvic resections. In: Proceedings of the 44th Annual International Conference of the IEEE Engineering in Medicine & Biology Society. EMBC, pp. 3481–3484. http://dx.doi.org/10.1109/EMBC48229.2022.9871766.

Meulstee, J.W., Nijsink, J., Schreurs, R., Verhamme, L.M., Xi, T., Delye, H.H.K., Borstlap, W.A., Maal, T.J.J., 2019. Toward holographic-guided surgery. Surg. Innov. 26, 86–94. http://dx.doi.org/10.1177/1553350618799552.

Moreta-Martinez, R., García-Mato, D., García-Sevilla, M., Pérez-Mañanes, R., Calvo-Haro, J.A., Pascau, J., 2020. Combining augmented reality and 3d printing to display patient models on a smartphone. J. Vis. Exp. 155, e60618. http://dx.doi.org/10.3791/60618.

Moreta-Martinez, R., Pose-Díez-de-la Lastra, A., Calvo-Haro, J.A., Mediavilla-Santos, L., Pérez-Mañanes, R., Pascau, J., 2021. Combining augmented reality and 3d printing to improve surgical workflows in orthopedic oncology: Smartphone application and clinical evaluation. Sensors-Basel 21, 1370. http://dx.doi.org/10.3390/s21041370.

Myers, P.L., Nelson, J.A., Rosen, E.B., Allen Jr, R.J., Disa, J.J., Matros, E., 2021. Virtual surgical planning for oncologic mandibular and maxillary reconstruction. Plast. Reconstr. Surg. 9, e3672. http://dx.doi.org/10.1097/GOX.0000000000003672.

Ohba, S., Kohara, H., Koga, T., Kawasaki, T., Miura, K.i., Yoshida, N., Asahina, I., 2017. Soft tissue changes after a mandibular osteotomy for symmetric skeletal class iii malocclusion. Odontology 105, 375–381. http://dx.doi.org/10.1007/s10266-016-0280-3.

Pavlíková, G., Foltán, R., Horká, M., Hanzelka, T., Borunská, H., Šedý, J., 2011. Piezosurgery in oral and maxillofacial surgery. Int. J. Oral Max. Surg. 40, 451–457. http://dx.doi.org/10.1016/j.ijom.2010.11.013.

Picón, M., Núñez, J., Almeida, F., 2021. Computer-assisted surgery in mandibular reconstruction. Innov. New Dev. Craniomaxillofac. Reconstr. 65–79. http://dx.doi.org/10.1007/978-3-030-74322-2_7.

Pietruski, P., Majak, M., Swiatek-Najwer, E., Zuk, M., Popek, M., Mazurek, M., Swiecka, M., Jaworowski, J., 2019. Supporting mandibular resection with intraoperative navigation utilizing augmented reality technology: A proof of concept study. J. Craniomaxillofac. Surg. 47, 854–859. http://dx.doi.org/10.1016/j.jcms.2019.03.004.

Pucci, R., Weyh, A., Smotherman, C., Valentini, V., Bunnell, A., Fernandes, R., 2020. Accuracy of virtual planned surgery versus conventional free-hand surgery for reconstruction of the mandible with osteocutaneous free flaps. Int. J. Oral Max. Surg. 49, 1153–1161. http://dx.doi.org/10.1016/j.ijom.2020.02.018.

Razali, N.M., Wah, Y.B., et al., 2011. Power comparisons of shapiro-wilk, kolmogorov-smirnov, lilliefors and anderson-darling tests. J. Stat. Model. Anal. 2, 21–33.

Resnick, C., 2018. Precise osteotomies for mandibular distraction in infants with robin sequence using virtual surgical planning. Int. J. Oral Max. Surg. 47, 35–43. http://dx.doi.org/10.1016/j.ijom.2017.07.020.

Sahovaler, A., Chan, H.H., Gualtieri, T., Daly, M., Ferrari, M., Vannelli, C., Eu, D., Manojlovic-Kolarski, M., Orzell, S., Taboni, S., et al., 2021. Augmented reality and intraoperative navigation in sinonasal malignancies: A preclinical study. Front. Oncol. 11, 723509. http://dx.doi.org/10.3389/fonc.2021.723509.

Salerno, F., Contenti, A., Ulrich, L., Marullo, G., Moos, S., Vezzetti, E., 2025. Mott modular optical tool tracking framework enabling efficient benchmarking. Sci. Rep. 15, 37205. http://dx.doi.org/10.1038/s41598-025-21044-z.

Salerno, F., Moos, S., Ulrich, L., Novaresio, A., Vezzetti, E., 2023. A methodology for the dimensional and mechanical analysis of surgical guides. In: International Conference of the Italian Association of Design Methods and Tools for Industrial Engineering. Springer, Cham, pp. 184–193. http://dx.doi.org/10.1007/978-3-031-52075-4_22.

Salerno, F., Ulrich, L., Maculotti, G., Moos, S., Genta, G., Vezzetti, E., Galetto, M., 2026. A metrological approach for augmented reality tooltip tracking assessment. Comput. Ind. 175, 104430. http://dx.doi.org/10.1016/j.compind.2025.104430.

García y Sánchez, J., Gómez Rodríguez, C., Romero Flores, J., 2015. Surgical guides for modified oblique le fort iii osteotomy. J. Maxillofac. Oral Surg. 14, 487–496. http://dx.doi.org/10.1007/s12663-014-0620-1.

Smatt, Y., Ferri, J., 2005. Retrospective study of 18 patients treated by maxillomandibular advancement with adjunctive procedures for obstructive sleep apnea syndrome. J. Craniofac. Surg. 16, 770–777. http://dx.doi.org/10.1097/01.scs.0000179746.98789.0f.

Sunil, T., Wolff, T.W., Scheker, L.R., McCabe, S.J., Gupta, A., 2006. A comparative study of ulnar-shortening osteotomy by the freehand technique versus the rayhack technique. J. Hand Surg. 31, 252–257. http://dx.doi.org/10.1016/j.jhsa.2005.09.017.

Tache, A., Mommaerts, M.Y., 2020. The need for maxillary osteotomy after primary cleft surgery: a systematic review framing a retrospective study. J. Craniomaxillofac. Surg. 48, 919–927. http://dx.doi.org/10.1016/j.jcms.2020.07.005.

Ulrich, L., Salerno, F., Moos, S., Vezzetti, E., 2024. How to exploit augmented reality (ar) technology in patient customized surgical tools: a focus on osteotomies. Multimedia Tools Appl. 1–32. http://dx.doi.org/10.1007/s11042-023-18058-y.

Vles, M., Terng, N., Zijlstra, K., Mureau, M., Corten, E., 2020. Virtual and augmented reality for preoperative planning in plastic surgical procedures: A systematic review. J. Plast. Reconstr. Aesthetic Surg. 73, 1951–1959. http://dx.doi.org/10.1016/j.bjps.2020.05.081.

Wang, Y., Zhang, H., Fan, S., Zhang, D., Huang, Z., Chen, W., Ye, J., Li, J., 2016. Mandibular reconstruction with the vascularized fibula flap: comparison of virtual planning surgery and conventional surgery. Int. J. Oral Max. Surg. 45, 1400–1405. http://dx.doi.org/10.1016/j.ijom.2016.06.015.

Weiss II, R.O., Ong, A.A., Reddy, L.V., Bahmanyar, S., Vincent, A.G., Ducic, Y., 2021. Orthognathic surgery—lefort i osteotomy. Facial Plast. Surg. 37, 703–708. http://dx.doi.org/10.1055/s-0041-1735308.

Westermark, A., Zachow, S., Eppley, B.L., 2005. Three-dimensional osteotomy planning in maxillofacial surgery including soft tissue prediction. J. Craniofac. Surg. 16, 100–104. http://dx.doi.org/10.1097/00001665-200501000-00019.

Xilloc, 2025. Surgical guides. https://www.xilloc.com/surgical-guides/. (Accessed 13 January 2025).

Xue, C., Xu, H., Tian, Y., Yang, X., Luo, E., Bai, D., 2018. Precise control of maxillary multidirectional movement in le fort i osteotomy using a surgical guiding device. Br. J. Oral Maxillofac. Surg. 56, 797–804. http://dx.doi.org/10.1016/j.bjoms.2018.08.013.

Zhao, R., Zhu, Z., Shao, L., Meng, F., Lei, Z., Li, X., Zhang, T., 2023. Augmented reality guided in reconstruction of mandibular defect with fibular flap: a cadaver study. J. Stomatol. Oral Maxillofac. Surg. 124, 101318. http://dx.doi.org/10.1016/j.jcms.2019.04.005.

Zhu, M., Liu, F., Chai, G., Pan, J.J., Jiang, T., Lin, L., Xin, Y., Zhang, Y., Li, Q., 2017. A novel augmented reality system for displaying inferior alveolar nerve bundles in maxillofacial surgery. Sci. Rep. 7, 42365. http://dx.doi.org/10.1038/srep42365.